

Cross Sections and Transverse Single-Spin Asymmetries in Forward Neutral-Pion Production from Proton Collisions at $\sqrt{s} = 200$ GeV

J. Adams,³ C. Adler,¹² M. M. Aggarwal,²⁵ Z. Ahammed,³⁸ J. Amonett,¹⁷ B. D. Anderson,¹⁷ M. Anderson,⁵ D. Arkhipkin,¹¹ G. S. Averichev,¹⁰ S. K. Badyal,¹⁶ J. Balewski,¹³ O. Barannikova,^{28,10} L. S. Barnby,³ J. Baudot,¹⁵ S. Bekele,²⁴ V. V. Belaga,¹⁰ R. Bellwied,⁴¹ J. Berger,¹² B. I. Bezverkhny,⁴³ S. Bhardwaj,²⁹ P. Bhaskar,³⁸ A. K. Bhati,²⁵ H. Bichsel,⁴⁰ A. Billmeier,⁴¹ L. C. Bland,² C. O. Blyth,³ B. E. Bonner,³⁰ M. Botje,²³ A. Boucham,³⁴ A. Brandin,²¹ A. Bravar,² R. V. Cadman,¹ X. Z. Cai,³³ H. Caines,⁴³ M. Calderón de la Barca Sánchez,² J. Carroll,¹⁸ J. Castillo,¹⁸ M. Castro,⁴¹ D. Cebra,⁵ P. Chaloupka,⁹ S. Chattopadhyay,³⁸ H. F. Chen,³² Y. Chen,⁶ S. P. Chernenko,¹⁰ M. Cherney,⁸ A. Chikanian,⁴³ B. Choi,³⁶ W. Christie,² J. P. Coffin,¹⁵ T. M. Cormier,⁴¹ J. G. Cramer,⁴⁰ H. J. Crawford,⁴ D. Das,³⁸ S. Das,³⁸ A. A. Derevschikov,²⁷ L. Didenko,² T. Dietel,¹² W. J. Dong,⁶ X. Dong,^{32,18} J. E. Draper,⁵ F. Du,⁴³ A. K. Dubey,¹⁴ V. B. Dunin,¹⁰ J. C. Dunlop,² M. R. Dutta Majumdar,³⁸ V. Eckardt,¹⁹ L. G. Efimov,¹⁰ V. Emelianov,²¹ J. Engelage,⁴ G. Eppley,³⁰ B. Erasmus,³⁴ M. Estienne,³⁴ P. Fachini,² V. Faine,² J. Faivre,¹⁵ R. Fatemi,¹³ K. Filimonov,¹⁸ P. Filip,⁹ E. Finch,⁴³ Y. Fisyak,² D. Flierl,¹² K. J. Foley,² J. Fu,⁴² C. A. Gagliardi,³⁵ N. Gagunashvili,¹⁰ J. Gans,⁴³ M. S. Ganti,³⁸ L. Gaudichet,³⁴ M. Germain,¹⁵ F. Geurts,³⁰ V. Ghazikhanian,⁶ P. Ghosh,³⁸ J. E. Gonzalez,⁶ O. Grachov,⁴¹ V. Grigoriev,²¹ S. Gronstal,⁸ D. Grosnick,³⁷ M. Guedon,¹⁵ S. M. Guertin,⁶ A. Gupta,¹⁶ E. Gushin,²¹ T. D. Gutierrez,⁵ T. J. Hallman,² D. Hardtke,¹⁸ J. W. Harris,⁴³ M. Heinz,⁴³ T. W. Henry,³⁵ S. Heppelmann,²⁶ T. Herston,²⁸ B. Hippolyte,⁴³ A. Hirsch,²⁸ E. Hjort,¹⁸ G. W. Hoffmann,³⁶ M. Horsley,⁴³ H. Z. Huang,⁶ S. L. Huang,³² T. J. Humanic,²⁴ G. Igo,⁶ A. Ishihara,³⁶ P. Jacobs,¹⁸ W. W. Jacobs,¹³ M. Janik,³⁹ H. Jiang,^{6,18} I. Johnson,¹⁸ P. G. Jones,³ E. G. Judd,⁴ S. Kabana,⁴³ M. Kaneta,¹⁸ M. Kaplan,⁷ D. Keane,¹⁷ V. Yu. Khodyrev,²⁷ J. Kiryluk,⁶ A. Kisiel,³⁹ J. Klay,¹⁸ S. R. Klein,¹⁸ A. Klyachko,¹³ D. D. Koetke,³⁷ T. Kollegger,¹² M. Kopytine,¹⁷ L. Kotchenda,²¹ A. D. Kovalenko,¹⁰ M. Kramer,²² P. Kravtsov,²¹ V. I. Kravtsov,²⁷ K. Krueger,¹ C. Kuhn,¹⁵ A. I. Kulikov,¹⁰ A. Kumar,²⁵ G. J. Kunde,⁴³ C. L. Kunz,⁷ R. Kh. Kutuev,¹¹ A. A. Kuznetsov,¹⁰ M. A. C. Lamont,³ J. M. Landgraf,² S. Lange,¹² C. P. Lansdell,³⁶ B. Lasiuk,⁴³ F. Laue,² J. Lauret,² A. Lebedev,² R. Lednický,¹⁰ M. J. LeVine,² C. Li,³² Q. Li,²² S. J. Lindenbaum,²² M. A. Lisa,²⁴ F. Liu,⁴² L. Liu,⁴² Z. Liu,⁴² Q. J. Liu,⁴⁰ T. Ljubicic,² W. J. Llope,³⁰ H. Long,⁶ R. S. Longacre,² M. Lopez-Noriega,²⁴ W. A. Love,² T. Ludlam,² D. Lynn,² J. Ma,⁶ Y. G. Ma,³³ D. Magestro,²⁴ S. Mahajan,¹⁶ L. K. Mangotra,¹⁶ D. P. Mahapatra,¹⁴ R. Majka,⁴³ R. Manweiler,³⁷ S. Margetis,¹⁷ C. Markert,⁴³ L. Martin,³⁴ J. Marx,¹⁸ H. S. Matis,¹⁸ Yu. A. Matulenko,²⁷ T. S. McShane,⁸ F. Meissner,¹⁸ Yu. Melnick,²⁷ A. Meschanin,²⁷ M. Messer,² M. L. Miller,⁴³ Z. Milosevich,⁷ N. G. Minaev,²⁷ C. Mironov,¹⁷ D. Mishra,¹⁴ J. Mitchell,³⁰ B. Mohanty,³⁸ L. Molnar,²⁸ C. F. Moore,³⁶ M. J. Mora-Corral,¹⁹ D. A. Morozov,²⁷ V. Morozov,¹⁸ M. M. de Moura,³¹ M. G. Munhoz,³¹ B. K. Nandi,³⁸ S. K. Nayak,¹⁶ T. K. Nayak,³⁸ J. M. Nelson,³ P. Nevski,² V. A. Nikitin,¹¹ L. V. Nogach,²⁷ B. Norman,¹⁷ S. B. Nurushev,²⁷ G. Odyniec,¹⁸ A. Ogawa,² V. Okorokov,²¹ M. Oldenburg,¹⁸ D. Olson,¹⁸ G. Paic,²⁴ S. U. Pandey,⁴¹ S. K. Pal,³⁸ Y. Panebratsev,¹⁰ S. Y. Panitkin,² A. I. Pavlinov,⁴¹ T. Pawlak,³⁹ V. Perevoztchikov,² C. Perkins,⁴ W. Peryt,³⁹ V. A. Petrov,¹¹ S. C. Phatak,¹⁴ R. Picha,⁵ M. Planinic,⁴⁴ J. Pluta,³⁹ N. Porile,²⁸ J. Porter,² A. M. Poskanzer,¹⁸ M. Potekhin,² E. Potrebenikova,¹⁰ B. V. K. S. Potukuchi,¹⁶ D. Prindle,⁴⁰ C. Pruneau,⁴¹ J. Putschke,¹⁹ G. Rai,¹⁸ G. Rakness,¹³ R. Raniwala,²⁹ S. Raniwala,²⁹ O. Ravel,³⁴ R. L. Ray,³⁶ S. V. Razin,^{10,13} D. Reichhold,²⁸ J. G. Reid,⁴⁰ G. Renault,³⁴ F. Retiere,¹⁸ A. Ridiger,²¹ H. G. Ritter,¹⁸ J. B. Roberts,³⁰ O. V. Rogachevski,¹⁰ J. L. Romero,⁵ A. Rose,⁴¹ C. Roy,³⁴ L. J. Ruan,^{32,2} R. Sahoo,¹⁴ I. Sakrejda,¹⁸ S. Salur,⁴³ J. Sandweiss,⁴³ I. Savin,¹¹ J. Schambach,³⁶ R. P. Scharenberg,²⁸ N. Schmitz,¹⁹ L. S. Schroeder,¹⁸ K. Schweda,¹⁸ J. Seger,⁸ D. Seliverstov,²¹ P. Seyboth,¹⁹ E. Shahaliev,¹⁰ M. Shao,³² M. Sharma,²⁵ K. E. Shestermanov,²⁷ S. S. Shimanskii,¹⁰ R. N. Singaraju,³⁸ F. Simon,¹⁹ G. Skoro,¹⁰ N. Smirnov,⁴³ R. Snellings,²³ G. Sood,²⁵ P. Sorensen,¹⁸ J. Sowinski,¹³ H. M. Spinka,¹ B. Srivastava,²⁸ S. Stanislaus,³⁷ R. Stock,¹² A. Stolpovsky,⁴¹ M. Strikhanov,²¹ B. Stringfellow,²⁸ C. Struck,¹² A. A. P. Suaide,³¹ E. Sugarbaker,²⁴ C. Suire,² M. Šumbera,⁹ B. Surrow,² T. J. M. Symons,¹⁸ A. Szanto de Toledo,³¹ P. Szarwas,³⁹ A. Tai,⁶ J. Takahashi,³¹ A. H. Tang,^{2,23} D. Thein,⁶ J. H. Thomas,¹⁸ V. Tikhomirov,²¹ M. Tokarev,¹⁰ M. B. Tonjes,²⁰ T. A. Trainor,⁴⁰ S. Trentalange,⁶ R. E. Tribble,³⁵ M. D. Trivedi,³⁸ V. Trofimov,²¹ O. Tsai,⁶ T. Ullrich,² D. G. Underwood,¹ G. Van Buren,² A. M. VanderMolen,²⁰ A. N. Vasiliev,²⁷ M. Vasiliev,³⁵ S. E. Vigdor,¹³ Y. P. Viyogi,³⁸ S. A. Voloshin,⁴¹ W. Wagoner,⁸ F. Wang,²⁸ G. Wang,¹⁷ X. L. Wang,³² Z. M. Wang,³² H. Ward,³⁶ J. W. Watson,¹⁷ R. Wells,²⁴ G. D. Westfall,²⁰ C. Whitten, Jr.,⁶ H. Wieman,¹⁸ R. Willson,²⁴ S. W. Wissink,¹³ R. Witt,⁴³ J. Wood,⁶ J. Wu,³² N. Xu,¹⁸ Z. Xu,² Z. Z. Xu,³² E. Yamamoto,¹⁸ P. Yepes,³⁰ V. I. Yurevich,¹⁰ Y. V. Zanevski,¹⁰ I. Zborovský,⁹ H. Zhang,^{43,2} W. M. Zhang,¹⁷ Z. P. Zhang,³² P. A. Żołnierczuk,¹³ R. Zoulkarneev,¹¹ J. Zoulkarneeva,¹¹ and A. N. Zubarev¹⁰

(STAR Collaboration)*

- ¹Argonne National Laboratory, Argonne, Illinois 60439, USA
²Brookhaven National Laboratory, Upton, New York 11973, USA
³University of Birmingham, Birmingham, United Kingdom
⁴University of California, Berkeley, California 94720, USA
⁵University of California, Davis, California 95616, USA
⁶University of California, Los Angeles, California 90095, USA
⁷Carnegie Mellon University, Pittsburgh, Pennsylvania 15213, USA
⁸Creighton University, Omaha, Nebraska 68178, USA
⁹Nuclear Physics Institute AS CR, Řež/Prague, Czech Republic
¹⁰Laboratory for High Energy (JINR), Dubna, Russia
¹¹Particle Physics Laboratory (JINR), Dubna, Russia
¹²University of Frankfurt, Frankfurt, Germany
¹³Indiana University, Bloomington, Indiana 47408, USA
¹⁴Institute of Physics, Bhubaneswar 751005, India
¹⁵Institut de Recherches Subatomiques, Strasbourg, France
¹⁶University of Jammu, Jammu 180001, India
¹⁷Kent State University, Kent, Ohio 44242, USA
¹⁸Lawrence Berkeley National Laboratory, Berkeley, California 94720, USA
¹⁹Max-Planck-Institut für Physik, Munich, Germany
²⁰Michigan State University, East Lansing, Michigan 48824, USA
²¹Moscow Engineering Physics Institute, Moscow Russia
²²City College of New York, New York City, New York 10031, USA
²³NIKHEF, Amsterdam, The Netherlands
²⁴Ohio State University, Columbus, Ohio 43210, USA
²⁵Panjab University, Chandigarh 160014, India
²⁶Pennsylvania State University, University Park, Pennsylvania 16802, USA
²⁷Institute of High Energy Physics, Protvino, Russia
²⁸Purdue University, West Lafayette, Indiana 47907, USA
²⁹University of Rajasthan, Jaipur 302004, India
³⁰Rice University, Houston, Texas 77251, USA
³¹Universidade de Sao Paulo, Sao Paulo, Brazil
³²University of Science & Technology of China, Anhui 230027, China
³³Shanghai Institute of Nuclear Research, Shanghai 201800, People's Republic of China
³⁴SUBATECH, Nantes, France
³⁵Texas A&M, College Station, Texas 77843, USA
³⁶University of Texas, Austin, Texas 78712, USA
³⁷Valparaiso University, Valparaiso, Indiana 46383, USA
³⁸Variable Energy Cyclotron Centre, Kolkata 700064, India
³⁹Warsaw University of Technology, Warsaw, Poland
⁴⁰University of Washington, Seattle, Washington 98195, USA
⁴¹Wayne State University, Detroit, Michigan 48201, USA
⁴²Institute of Particle Physics, CCNU (HZNU), Wuhan, 430079 China
⁴³Yale University, New Haven, Connecticut 06520, USA
⁴⁴University of Zagreb, Zagreb, HR-10002, Croatia

(Received 3 November 2003; published 29 April 2004)

Measurements of the production of forward high-energy π^0 mesons from transversely polarized proton collisions at $\sqrt{s} = 200$ GeV are reported. The cross section is generally consistent with next-to-leading order perturbative QCD calculations. The analyzing power is small at x_F below about 0.3, and becomes positive and large at higher x_F , similar to the trend in data at $\sqrt{s} \leq 20$ GeV. The analyzing power is in qualitative agreement with perturbative QCD model expectations. This is the first significant spin result seen for particles produced with $p_T > 1$ GeV/c at a polarized proton collider.

DOI: 10.1103/PhysRevLett.92.171801

PACS numbers: 13.85.Ni, 12.38.Qk, 13.88.+e

An early qualitative expectation from perturbative quantum chromodynamics (pQCD) was that the chiral properties of the theory would make the analyzing power

for inclusive particle production be very small [1]. The analyzing power (A_N) is the azimuthal asymmetry in particle yields from a transversely polarized beam

incident on an unpolarized target. Earlier experiments studied polarized proton collisions ($p_{\uparrow} + p$) at center-of-mass energies $\sqrt{s} \leq 20$ GeV and measured A_N for pion production at moderate transverse momentum ($0.5 \leq p_T \leq 2.0$ GeV/ c). Contrary to the naive expectation, A_N was found to be 20%–40% for pions produced at large values of Feynman x ($x_F = 2p_L/\sqrt{s}$, where p_L is the longitudinal momentum of the pion) [2–5]. Similarly, elastic proton [6] and recent semi-inclusive deep-inelastic lepton scattering experiments [7,8] have reported transverse single-spin asymmetries which differ significantly from zero. These results have sparked substantial theoretical activity to understand transverse spin effects within the framework of pQCD [9].

Perturbative QCD calculations of pion production involve the convolution of parton distribution and fragmentation functions with a hard partonic interaction. The reliability of calculations in the pQCD framework is expected to increase with p_T . In this framework, forward π production in $p + p$ collisions is dominated by scattering of a valence quark in one proton from a soft gluon in the other. At large pseudorapidities (η) and $\sqrt{s} \leq 20$ GeV, there may be significant contributions to particle production from soft hadronic processes collectively known as beam fragmentation. At a collider, \sqrt{s} is significantly larger, leading to the expectation that the origin of forward pions will shift towards collisions of the partonic constituents of the proton, consistent with the PYTHIA Monte Carlo generator [10]. Measurements of the cross section for forward pion production are important to establish that pQCD is a suitable framework for treating polarization observables in these kinematics.

Different mechanisms have been identified in the pQCD framework by which one might expect transverse spin effects [11–17], all of which may contribute to some degree. With only data at $\sqrt{s} \leq 20$ GeV for comparison, these models are not well constrained. Despite this, the models have been extrapolated by an order of magnitude in \sqrt{s} and approximately a factor of 2 in p_T , and all predict that sizable transverse spin effects will persist at $\sqrt{s} = 200$ GeV. This Letter addresses the question if A_N is sizable at $\sqrt{s} = 200$ GeV, as predicted by these models. We present measurements of the cross section and A_N for the production of forward π^0 mesons having $p_T > 1$ GeV/ c from $p_{\uparrow} + p$ collisions at $\sqrt{s} = 200$ GeV.

Data were collected by the STAR experiment (Solenoid Tracker at RHIC) at the Brookhaven National Laboratory Relativistic Heavy Ion Collider (RHIC) in January 2002. RHIC is the first polarized proton collider. Polarization is produced by optical pumping of an atomic-beam source [18] and is partially preserved through an accelerator complex to reach RHIC [19]. In RHIC, a pair of helical dipole magnets in each ring serves as the first use of full “Siberian snakes” [20] in a high-energy accelerator to preserve polarization during beam acceleration. The stable spin axis of the RHIC rings is vertical. Beam

bunches crossed the STAR interaction region (IR) every 213 ns. The polarization direction alternated between up and down for successive bunches of one beam and after every two bunches of the other beam. Data were sorted according to the spin direction of the beam corresponding to positive x_F pion production. Summing all bunches in the other beam resulted in negligible remnant polarization. Typical luminosities were 10^{30} cm $^{-2}$ s $^{-1}$, and the integrated luminosity was 150 nb $^{-1}$ for these data.

The average beam polarization for each fill, P_{beam} , was determined using a Coulomb-Nuclear Interference (CNI) polarimeter located in RHIC [21,22]. At 24.3 GeV, the RHIC injection energy, the analyzing power of the CNI reaction is $A_N^{\text{CNI}} = 0.0133 \pm 0.0041$ [23,24], and can be used to deduce the absolute polarization of the proton beam. However, at 100 GeV, the beam energy used for RHIC collisions, A_N^{CNI} has not yet been measured. The CNI asymmetries measured at injection and collision energies were nearly equal for many fills. Since the beam acceleration process is unlikely to increase P_{beam} , this suggests that A_N^{CNI} at 100 GeV is no smaller than at 24.3 GeV. For the present analysis, we assume there is no change in A_N^{CNI} between these two energies, giving an average value of $\langle P_{\text{beam}} \rangle = 0.16$.

A prototype forward π^0 detector (PFPD) was installed at STAR 750 cm from the IR to identify π^0 mesons. At this time, STAR does not have the capability to identify large rapidity charged pions. The PFPD consisted of a Pb-scintillator sampling calorimeter [25], placed with its edge ≈ 30 cm left of the oncoming polarized proton beam (beam left). The PFPD was 21 radiation lengths deep and subdivided into 4×3 towers. To measure the transverse profiles of photon showers, the PFPD had a shower-maximum detector (SMD) approximately 5 radiation lengths deep, comprising two orthogonal layers of 100×60 scintillator strips spaced at 0.37 cm. To address systematic errors associated with measuring left-right asymmetries with a single arm detector, an array of Pb-glass detectors with no SMD was placed to the right of the oncoming polarized proton beam (beam right). Similar arrays were placed above and below the vertically polarized beam, where no asymmetries are expected.

The luminosity was measured at STAR using beam-beam counters (BBC) [26] composed of segmented scintillator annuli mounted around the beam at longitudinal positions $z = \pm 370$ cm, spanning $3.3 < |\eta| < 5.0$. Proton collision events were identified by requiring the coincidence of at least one BBC segment fore and aft of the IR. Absolute luminosity was determined by measuring the transverse size of the colliding beams and the number of protons colliding at STAR. The cross section measured for the BBC coincidence condition is $26.1 \pm 0.2(\text{stat}) \pm 1.8(\text{syst})$ mb [27], consistent with simulation [10,28]. The BBC observes $87\% \pm 8\%$ of the inelastic, nonsingly diffractive cross section.

All forward calorimeters were read out when the energy deposited in any one calorimeter was greater than that from an electron of ~ 15 GeV. The BBC coincidence requirement was imposed to select $p + p$ collisions.

The asymmetry measured at beam left is

$$P_{\text{beam}} A_N = \frac{N_+ - RN_-}{N_+ + RN_-}. \quad (1)$$

The number of π^0 mesons detected when the beam spin vector was oriented up (down) is $N_{+(-)}$. The spin-dependent relative luminosity ($R = \mathcal{L}_+ / \mathcal{L}_- \approx 1.15$) was measured with the BBC. Background contributions to R were reduced by increasing the coincidence requirements to at least two BBC segments on each side of STAR. The systematic errors on R , primarily coming from the change in R when the background is corrected, are of the order of 10^{-3} [26] and are a factor of 10 to 20 smaller than $P_{\text{beam}} A_N$ measured with the PFPD.

Neutral pions are reconstructed utilizing the formula $M_{\gamma\gamma} = E_{\pi} \sqrt{1 - z_{\gamma}^2} \sin(\phi_{\gamma\gamma}/2) \approx E_{\text{tot}} \sqrt{1 - z_{\gamma}^2} d_{\gamma\gamma} / 2z_{\text{vtx}}$ using events with at least two clusters in the SMD. The energy of the leading π^0 , E_{π} , is taken to be the total energy deposited in all of the towers, E_{tot} . The opening angle between the two photons, $\phi_{\gamma\gamma}$, is determined by z_{vtx} , the distance between the collision vertex and the PFPD, and the separation of the photons at the detector, $d_{\gamma\gamma}$. Both $d_{\gamma\gamma}$ and $z_{\gamma} = |E_{\gamma 1} - E_{\gamma 2}| / (E_{\gamma 1} + E_{\gamma 2})$ are measured by an analysis of the energy deposited in the strips of the SMD. The value of $d_{\gamma\gamma}$ is determined from the fitted centroids of the peaks, while z_{γ} is derived from the ratio of the fitted areas under the peaks. A fiducial volume is defined by requiring the SMD peaks to be more than 12 strips from the detector edge. Figure 1 shows the $M_{\gamma\gamma}$ spectra for two energy bins. The mass resolution is $20 \text{ MeV}/c^2$ (rms) for $15 < E_{\text{tot}} < 80$ GeV, limited by the measurement of $\phi_{\gamma\gamma}$. The centroid of the π^0 peak is used to determine the calibration for each tower for each fill to an accuracy of the order of 1%. The calibration is found to have negligible dependence on energy or spin state.

The π^0 detection efficiency is determined in a matrix of E_{π} and η from a Monte Carlo (MC) simulation of $p + p$ collisions [10] and the detector response [28]. The open histograms in Fig. 1 are MC events which undergo the same reconstruction and selection as the data. The MC matches the data well for several variables, including p_T , E_{tot} , and η . The π^0 detection efficiency is dominated by the geometrical acceptance of the calorimeter.

The π^0 sample is distorted by coincident particles from the jets containing them. The PFPD is about one hadronic interaction length deep. When two photons from π^0 decay overlap with other particles, the PFPD response to the other particles tends to increase E_{tot} relative to E_{π} and broaden the $\phi_{\gamma\gamma}$ resolution. This results in a broad $M_{\gamma\gamma}$ distribution peaked at a value larger than M_{π} . The average value of E_{tot} is about 3 GeV larger than E_{π} , indepen-

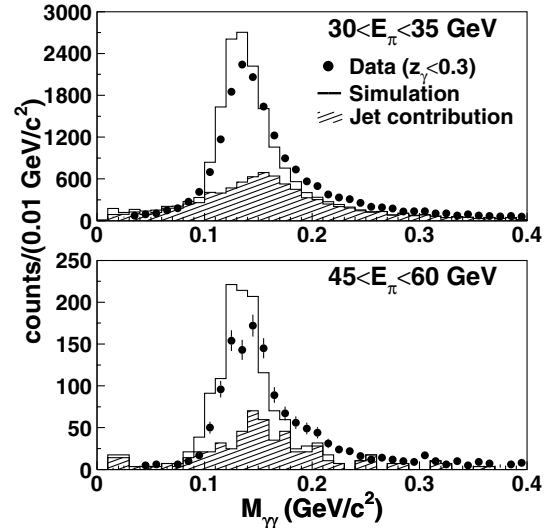


FIG. 1. Uncorrected spectra of the diphoton invariant mass in two energy bins. The points are data with statistical errors. The open histograms are reconstructed simulation events, normalized to equal area. The hatched histograms are used to correct the cross section.

dent of E_{π} . MC events with $|E_{\text{tot}} - E_{\pi}| > 2$ GeV are shown as the hatched histograms in Fig. 1. Events with only one photon from π^0 decay plus other particles exist predominantly at small $M_{\gamma\gamma}$, and are suppressed by requiring $z_{\gamma} < 0.3$. The E_{π} -dependent systematic error in the cross section is about 20%, dominated by the jet correction. The MC simulation includes π^0 events from forward jets. The uncertainty includes the difference when these effects are explicitly corrected in both the data and the simulation, and in neither.

Noncollision background is suppressed to the level of 1% by requiring the coincidence from the BBC in the offline analysis. Following our simulations, the cross section is corrected by 10% to account for the bias introduced by the BBC coincidence condition. Hadronic background comprising events with no leading π^0 in the acceptance of the calorimeter is predominantly at small $M_{\gamma\gamma}$, and is reduced by constraining z_{γ} . The hadronic background amounts to about 2% of the yield underneath the π^0 peak at $0.09 < M_{\gamma\gamma} < 0.22 \text{ GeV}/c^2$.

The inclusive π^0 production cross section for $30 < E_{\pi} < 55$ GeV in 5 GeV bins is presented in Fig. 2. Data with $3.4 < \eta < 4.0$ were selected, giving $\langle \eta \rangle = 3.8$ independent of E_{π} ; in this range the detector efficiency is well understood. The dominant contributions to the normalization error come from knowledge of the absolute transverse position of the detector (10%), the absolute luminosity determination (8%), and the model dependence of the BBC efficiency (8%). The data are plotted at the average E_{π} of the bin.

The curves on the plot are next-to-leading order (NLO) pQCD calculations [29] evaluated at $\eta = 3.8$, using the CTEQ6M [32] parton distribution functions and equal

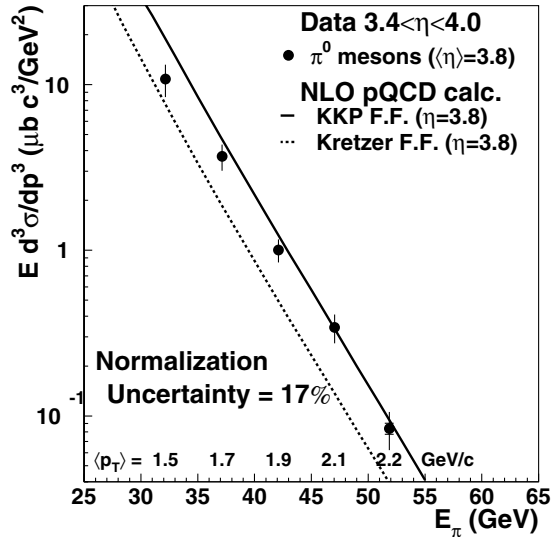


FIG. 2. Inclusive π^0 production cross section versus leading π^0 energy (E_π). The average transverse momentum ($\langle p_T \rangle$) is correlated with E_π , as the PFPD was at a fixed pseudorapidity (η). The inner error bars are statistical, and are smaller than the symbols for most points. The outer error bars combine these with the E_π -dependent systematic errors. The curves are NLO pQCD calculations evaluated at $\eta = 3.8$ [29–31].

renormalization and factorization scales of p_T . The NLO pQCD calculations are in general consistent with the data, in contrast to midrapidity π^0 data at lower \sqrt{s} [33]. The solid line uses the “Kniehl-Kramer-Pötter” (KKP) set of fragmentation functions (FF) [30], while the dashed line uses the “Kretzer” set [31]. The difference between the two reflects uncertainties in the FF at these kinematics. At the chosen scale, KKP tends to agree with the data better than Kretzer, consistent with midrapidity π^0 data at $\sqrt{s} = 200$ GeV [34].

The analyzing power is presented in Fig. 3, plotted versus $2\langle E_{\text{tot}} \rangle / \sqrt{s} \approx x_F$. The solid points are for π^0 mesons from $3.3 < \eta < 4.1$ and $0.07 < M_{\gamma\gamma} < 0.3$ GeV/ c^2 , with x_F -dependent constraints on z_γ to minimize background. The open points are based solely on E_{tot} in the PFPD without SMD analysis: neither fiducial volume constraints nor π^0 identification. The agreement between the solid and open points indicates A_N is not sensitive to the analysis used to identify π^0 mesons. This is consistent with simulations showing that 95% of events with at least 25 GeV deposited in the PFPD come from photons, 95% of which are daughters from π^0 decay. The A_N seen at beam right with the Pb-glass array is similar to that seen at beam left with the PFPD, while A_N for the Pb-glass above and below the beam is consistent with zero, as expected. The largest x_F -dependent systematic error arises from comparison of the beam-left and beam-right data. The average $A_N(x_F)$ is computed using both, and an uncertainty is assigned to bring $A_N(x_F)$ (shown in Fig. 3) within 1 standard deviation of the average.

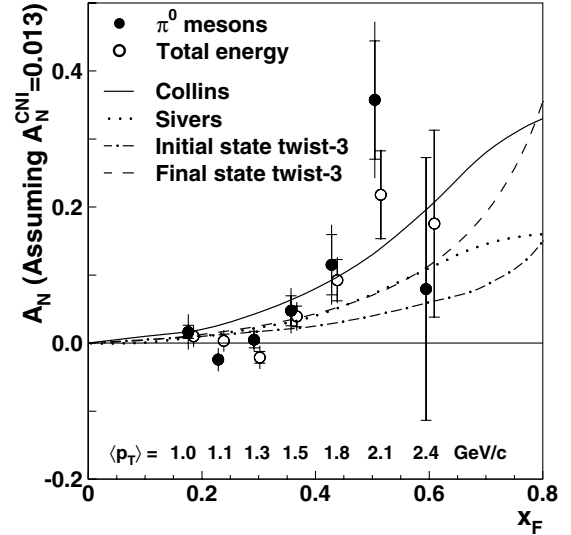


FIG. 3. Analyzing powers versus Feynman x (x_F). The average transverse momentum ($\langle p_T \rangle$) is correlated with x_F . The solid points are for identified π^0 mesons. The open points are for the total energy (E_{tot}), shifted by $x_F + 0.01$. The inner error bars are statistical, and the outer combine these with the point-to-point systematic errors. The curves are from pQCD models evaluated at $p_T = 1.5$ GeV/ c [14–17]. The A_N values are proportional to A_N^{CNI} , assumed to be 0.013 at 100 GeV.

The curves on the plot are predictions from the pQCD models, fitted to data at $\sqrt{s} = 20$ GeV, extrapolated to $\sqrt{s} = 200$ GeV and evaluated at $p_T = 1.5$ GeV/ c [14–17]. One model attributes single-spin effects to the convolution of the transversity distribution function with a spin-dependent Collins fragmentation function [14]. The Sivvers model adds explicit spin-dependent k_T dependence to the parton distribution functions [15]. Other models ascribe the effects to twist-3 parton correlations in the initial or final state [16,17]. The data are qualitatively consistent with all of these predictions.

The trend of A_N at lower \sqrt{s} is to increase from zero beginning at a value of x_F which depends on \sqrt{s} [5]. The significance of the increase for these data is 4.7σ (including statistical and point-to-point systematic errors) from a linear fit to the open circles in Fig. 3 for $x_F > 0.27$, with $\chi^2 = 0.9$ for 3 degrees of freedom. This is the first significant spin result seen for particles with $p_T > 1$ GeV/ c at a polarized proton collider.

In summary, high-energy π^0 mesons have been observed at forward angles from $p_1 + p$ collisions at $\sqrt{s} = 200$ GeV. The differential cross section is, in general, consistent with NLO pQCD calculations. The analyzing power is small at x_F below about 0.3, and becomes positive and large at higher x_F , similar to the trend observed in fixed-target data at $\sqrt{s} \leq 20$ GeV. The analyzing power at $\sqrt{s} = 200$ GeV is in qualitative agreement with pQCD model predictions. Higher precision measurements of A_N as a function of both x_F and p_T may help to

differentiate among the models. Future measurements may attempt to determine the Collins fragmentation function in $p_1 + p$ collisions, as well as to look at jet production and Drell-Yan scattering to isolate potential contributions to transverse spin effects.

We thank the RHIC Operations Group and RCF at BNL, and the NERSC Center at LBNL for their support. This work was supported in part by the HENP Divisions of the Office of Science of the U.S. DOE; the U.S. NSF; the BMBF of Germany; IN2P3, RA, RPL, and EMN of France; EPSRC of the United Kingdom; FAPESP of Brazil; the Russian Ministry of Science and Technology; the Ministry of Education and the NNSFC of China; Grant Agency of the Czech Republic, DAE, DST, and CSIR of the Government of India; the Swiss NSF.

*URL: www.star.bnl.gov

- [1] G. L. Kane, J. Pumplin, and W. Repko, Phys. Rev. Lett. **41**, 1689 (1978).
- [2] R. D. Klem *et al.*, Phys. Rev. Lett. **36**, 929 (1976); W. H. Dragoset *et al.*, Phys. Rev. D **18**, 3939 (1978).
- [3] S. Saroff *et al.*, Phys. Rev. Lett. **64**, 995 (1990); B. E. Bonner *et al.*, Phys. Rev. D **41**, 13 (1990).
- [4] B. E. Bonner *et al.*, Phys. Rev. Lett. **61**, 1918 (1988); A. Bravar *et al.*, *ibid.* **77**, 2626 (1996); D. L. Adams *et al.*, Phys. Lett. B **261**, 201 (1991); **264**, 462 (1991); Z. Phys. C **56**, 181 (1992).
- [5] K. Krueger *et al.*, Phys. Lett. B **459**, 412 (1999); C. E. Allgower *et al.*, Phys. Rev. D **65**, 092008 (2002).
- [6] P. R. Cameron *et al.*, Phys. Rev. D **32**, 3070 (1985); D. G. Crabb *et al.*, Phys. Rev. Lett. **65**, 3241 (1990).
- [7] A. Airapetian *et al.*, Phys. Rev. Lett. **84**, 4047 (2000); Phys. Lett. B **535**, 85 (2002); **562**, 182 (2003).
- [8] A. Bravar *et al.*, Nucl. Phys. Proc. Suppl. **79**, 520 (1999).
- [9] For a review, see V. Barone, A. Drago, and P. G. Ratcliffe, Phys. Rep. **359**, 1 (2002).
- [10] T. Sjöstrand, Comput. Phys. Commun. **82**, 74 (1994).
- [11] J. Collins, Nucl. Phys. **B396**, 161 (1993).
- [12] D. Sivers, Phys. Rev. D **41**, 83 (1990); **43**, 261 (1991).
- [13] A. Efremov and O. Teryaev, Phys. Lett. **150B**, 383 (1985).
- [14] M. Anselmino, M. Boglione, and F. Murgia, Phys. Rev. D **60**, 054027 (1999); M. Boglione and E. Leader, Phys. Rev. D **61**, 114001 (2000).
- [15] M. Anselmino, M. Boglione, and F. Murgia, Phys. Lett. B **362**, 164 (1995); M. Anselmino and F. Murgia, *ibid.* **442**, 470 (1998); U. D'Alesio and F. Murgia, AIP Conf. Proc. **675**, 469 (2003).
- [16] J. Qiu and G. Sterman, Phys. Rev. D **59**, 014004 (1998).
- [17] Y. Koike, AIP Conf. Proc. **675**, 449 (2003).
- [18] A. Zelenski *et al.*, in *Proceedings of the Particle Acceleration Conference* (IEEE, New York, 1999), p. 106.
- [19] G. Bunce *et al.*, Annu. Rev. Nucl. Part. Sci. **50**, 525 (2000); H. Huang *et al.*, Phys. Rev. Lett. **73**, 2982 (1994); M. Bai *et al.*, *ibid.* **80**, 4673 (1998).
- [20] Ya. S. Derbenev *et al.*, Part. Accel. **8**, 115 (1978).
- [21] I. G. Alekseev *et al.*, AIP Conf. Proc. **675**, 812 (2003).
- [22] H. Spinka, AIP Conf. Proc. **675**, 807 (2003).
- [23] O. Jinnouchi *et al.*, AIP Conf. Proc. **675**, 817 (2003).
- [24] J. Tojo *et al.*, Phys. Rev. Lett. **89**, 052302 (2002).
- [25] C. Allgower *et al.*, Nucl. Instrum. Methods Phys. Res., Sect. A **499**, 740 (2003).
- [26] J. Kiryluk, AIP Conf. Proc. **675**, 424 (2003).
- [27] J. Adams *et al.*, Phys. Rev. Lett. **91**, 172302 (2003); A. Drees and Z. Xu, in *Proceedings of the Particle Acceleration Conference* (IEEE, Chicago, IL, 2001), p. 3120.
- [28] GEANT 3.21, CERN program library.
- [29] F. Aversa *et al.*, Nucl. Phys. **B327**, 105 (1989); B. Jager *et al.*, Phys. Rev. D **67**, 054005 (2003); D. de Florian, *ibid.* **67**, 054004 (2003).
- [30] B. A. Kniehl *et al.*, Nucl. Phys. **B597**, 337 (2001).
- [31] S. Kretzer, Phys. Rev. D **62**, 054001 (2000).
- [32] J. Pumplin *et al.*, J. High Energy Phys. **07** (2002) 012.
- [33] P. Aurenche *et al.*, Eur. Phys. J. C **13**, 347 (2000).
- [34] S. S. Adler *et al.*, Phys. Rev. Lett. **91**, 241803 (2003).